XLI CILAMCE
XLI Ibero-Latin American Congress on Computational Methods in Engineering
16-19 November, 2020 FOZ DO IGUAÇU PARANÁ - BRAZIL

COMPUTATIONAL MODEL FOR A POLYMER EXTRUDER SCREW

Matheus Rocha Ferrari [1], Dianne Magalhães Viana [1], Adriano Possebon Rosa[1]

[1]*Dept. of Mechanical Engineering , University of Brasília*
UnB - Brasília, Distrito Federal, Brasil, 70910-900
matheus.rochaf2@gmail.com, diannemv@unb.br, aprosa@unb.br

Abstract.

The most adequate process for an extrusive screw is the condition of operation. That involves the type of polymer, the flow rate, mixture devices, temperature control and die. In view of productivity demands, e.g. flow speed and filament homogeneity, it is deemed necessary a detailed study on the behaviour of the polymer along the screw. This work aims at the development of a computational model, a tool which will be used on the design of the screw of the extruder machine. Our model seeks to simulate the behavior of the material, providing enough information for an adequate design for the screw, which is necessary in order to define the parameter for a viable production.

The implemented model is based on the conservation of energy and moment equations, for which numerical solutions are obtained through a projection method, where different boundary conditions are used for distinct stages of the processes - feeding, metering and dosage. We simplify the process by considering a steady state regime on a bi-dimensional domain. This characterizes a classical cavity problem. Since a rise of root diameter along the axis is observed on most of commercial screws, this was the standard geometry adopted for the model. After numerically solving the 2D Navier-Stokes equations, the pressure and velocity of the flow, which are obtained for every stage, allow us to assess the efficiency of the process for the given geometry.

Keywords: Projection method, lid-driven cavity, Navier-Stokes, extruder screw, finite differences

1 Introduction

Numerical solutions of the Navier-Stokes equations are widely studied in the field of computational fluid dynamics (CFD), powered by the numerous applicabilities in physics and engineering. It is an important tool to study the behavior of both Newtonian and non-Newtonian fluids, and many of the polymers in the plastic processing industry are in the category of the latter.

This paper aims to simulate a polymer inside a single-screw extruder machine by elaborating a model capable of obtaining a solution to the Navier-Stokes equations for a non-Newtonian fluid in a time dependent lid-driven cavity problem. There are many models that can describe, with good precision, the physical behavior of this flow. Due to characteristics of the physical geometry of the channel in which the polymer must go through, we are able to simplify the domain of our model into a two-dimensional Cartesian coordinate system from what would usually be parameterized by a three-dimensional cylindrical one.

One of the main difficulties in this type of problem is to uncouple the velocity from the pressure, a relationship which is imposed by the incompressibility restriction. We circumvent this obstacle by making use of the projection method, which has been widely studied in the literature and shown to be an efficient numerical scheme for the incompressible flow, as first seen in the work of Chorin [1]. In order to evaluate the accuracy and efficiency of the numerical method, a comparison with benchmark works can be done, since lid-driven cavity problems are broadly studied and used to validate some standard operation conditions. Based on the dependence of the viscosity on the shear-rates, the fluid can be described as Newtonian or non-Newtonian fluid. In our case, when dealing with a non-Newtonian, more complex constitutive equations for the model arise if compared to the Newtonian equations, but they can be described by the shear-thinning or shear-thickening characteristics of the fluid when using a power-law model.

2 Theory

2.1 Physical Model

The physical modeling seeks to simulate, in a simplified way, the phenomena that occurs inside an single screw extruder. With this purpose, the fluid is taken as a non-Newtonian power law fluid and a few geometry simplifications are made.

Inside an extruder machine, the polymer goes through a channel, created by the screw and the barrel of the extruder (Fig. 1).

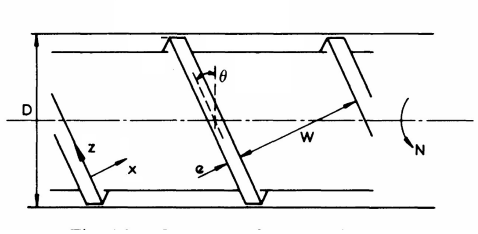

Figure 1. Geometry of an extruder screw, from Richard and Pearson [2]

This helical channel has a width, w, a heigth, H, and an angle, θ. The screw channel is relatively shallow, and it is reasonable to assume that the channel may be unrolled and treated as rectilinear (cite FENNER). Cartesian coordinates were adopted for this problem, fixed to a stationary screw. This way, the upper wall is the driven wall. The unrolled channel is treated as a three-dimensional cavity and the upper wall slides diagonally, with a velocity component in x and z directions (Fig. 2).

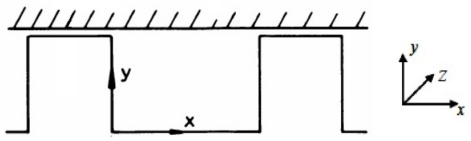

Figure 2. View down screw channel in the positive x direction, from Richard and Pearson [2], with adaptations.

With the purpose of comparison with benchmark problems, such as lid-driven cavity with a power-law viscosity model, the velocity in z is disregarded. This way, the influence of the velocity of the upper border and flow behavior index in the streamlines and pressure field become more prominent.

2.2 Mathematical Model

The model was created to simulate an incompressible fluid, ruled by the Navier-Stokes and energy equations, with a shear-rate dependant viscosity. This governing equations are presented below, in the dimensional form.

$$\frac{\partial u}{\partial x} + \frac{\partial v}{\partial y} = 0 \tag{1}$$

$$\frac{\partial u}{\partial t} + u\frac{\partial u}{\partial x} + v\frac{\partial u}{\partial y} = -\frac{\partial p}{\partial x} + \frac{\partial}{\partial x}\left(2\mu\frac{\partial u}{\partial x}\right) + \frac{\partial}{\partial y}\left(\mu\frac{\partial u}{\partial y}\right) + \frac{\partial}{\partial y}\left(\mu\frac{\partial v}{\partial x}\right) \tag{2}$$

$$\frac{\partial v}{\partial t} + u\frac{\partial v}{\partial x} + v\frac{\partial v}{\partial y} = -\frac{\partial p}{\partial y} + \frac{\partial}{\partial x}\left(\mu\frac{\partial v}{\partial x}\right) + \frac{\partial}{\partial y}\left(2\mu\frac{\partial v}{\partial y}\right) + \frac{\partial}{\partial x}\left(\mu\frac{\partial u}{\partial y}\right) \tag{3}$$

In the power-law model, the apparent viscosity, μ, is a function of the shear-rate, given by

$$\mu = \mu_0|\dot{\gamma}|^{(n-1)} \tag{4}$$

where μ_0 is the flow consistency, $\dot{\gamma}$ is the second invariant of the rate-of-strain tensor, n is the flow behavior index.

The behavior of a non-Newtonian fluid can be simulated in a very approximated way using the eq.(4). The flow behavior index , n, changes the characteristics of the viscosity. In the range $n < 1$, the viscosity is shear-thinning and in range $n > 1$, the viscosity is shear-thickening.

For bi-dimensional flow, the shear-rate is given by

$$|\dot{\gamma}| = \sqrt{2\left(\frac{\partial u}{\partial x}\right)^2 + 2\left(\frac{\partial v}{\partial y}\right)^2 + \left(\frac{\partial u}{\partial y} + \frac{\partial v}{\partial x}\right)^2}. \tag{5}$$

In order to non-dimensionalize the equations 1, 2 and 3, the variables were used as follows

$$x^* = \frac{x}{H}, \quad y^* = \frac{y}{H}, \quad p^* = \frac{p}{\rho {u_0}^2}, \quad t^* = \frac{t u_0}{H}, \quad u^* = \frac{u}{u_0}, \quad v^* = \frac{v}{u_0}, \tag{6}$$

$$Re = \frac{{u_0}^{n-2} H^n}{\nu_0}, \quad \nu_0 = \frac{\mu_0}{\rho}, \quad D = \frac{\mu}{\mu_0}. \tag{7}$$

Using the variables described previously, without the asteristik symbol (*), the non-dimensional form of the governing equations can be written as

$$\frac{\partial u}{\partial x} + \frac{\partial v}{\partial y} = 0 \tag{8}$$

$$\frac{\partial u}{\partial t} + u\frac{\partial u}{\partial x} + v\frac{\partial u}{\partial y} = -\frac{\partial p}{\partial x} + \frac{1}{Re}\frac{\partial}{\partial x}\left(2D\frac{\partial u}{\partial x}\right) + \frac{1}{Re}\frac{\partial}{\partial y}\left(D\frac{\partial u}{\partial y}\right) + \frac{1}{Re}\frac{\partial}{\partial y}\left(D\frac{\partial v}{\partial x}\right) \tag{9}$$

$$\frac{\partial v}{\partial t} + u\frac{\partial v}{\partial x} + v\frac{\partial v}{\partial y} = -\frac{\partial p}{\partial y} + \frac{1}{Re}\frac{\partial}{\partial x}\left(D\frac{\partial v}{\partial x}\right) + \frac{1}{Re}\frac{\partial}{\partial y}\left(2D\frac{\partial v}{\partial y}\right) + \frac{1}{Re}\frac{\partial}{\partial x}\left(D\frac{\partial u}{\partial y}\right) \tag{10}$$

where *D* is the non-dimensional fluid viscosity following the power-law model, proposed in the work of Molla and Yao [3].

$$D = \begin{cases} 1 & \text{if} \quad |\dot{\gamma}| < \gamma_1 \\ |\dot{\gamma}|^{n-1} & \text{if} \quad \gamma_1 \leq |\dot{\gamma}| \leq \gamma_2 \\ \gamma_2^{n-1} & \text{if} \quad |\dot{\gamma}| > \gamma_2. \end{cases} \tag{11}$$

The constants γ_1 and γ_2 are the threshold shear-rates ($\gamma_1 = 10^{-2}$ and $\gamma_2 = 10^5$). The eq. (11) describes that the range, in which the non-dimensional viscosity is well approximated, lies between the thresholds γ_1 and γ_2.

3 Methodology

To solve the proposed equations, the projection method is used [1]. In this method, the restrictions of incompressibility and the Navier-Stokes equations are solved in a non-simultaneous way. At the beginning, the incompressibility restriction is ignored and a u^* velocity is calculated from the Navier-Stokes equation (without the pressure term).

$$\frac{u^* - u^k}{dt} + u^k \cdot \nabla u^k = \frac{1}{Re}\frac{\partial}{\partial x}\left(2D\frac{\partial u}{\partial x}\right) + \frac{1}{Re}\frac{\partial}{\partial y}\left(D\frac{\partial u}{\partial y}\right) + \frac{1}{Re}\frac{\partial}{\partial y}\left(D\frac{\partial v}{\partial x}\right) \tag{12}$$

The following equation is used to calculate the pressure term, using u^*.

$$\nabla^2 p^{k+1} = \frac{1}{dt}\nabla \cdot u^* \tag{13}$$

The term of velocity that is related to a step forward in time (u^{k+1}) can be calculated as follow

$$u^{k+1} = u^* - dt\nabla p^{k+1}. \tag{14}$$

3.1 Boundary Conditions

The boundary conditions are of extreme importance, influencing the accuracy and stability of the numerical method. For the velocity, the no-slip boundary condition is considered, and it can be expressed as

$$v(x = 0, y) = 0, \quad v(x = 1, y) = 0, \quad u(x, y = 0) = 0, \quad u(x, y = 1) = u_0. \tag{15}$$

The Neumann Boundary condition is used, in which the normal derivative of the pressure is null, i.e.

$$\frac{\partial p}{\partial \mathbf{n}} = 0 \tag{16}$$

The origin of the system can be seen in Fig. 3.

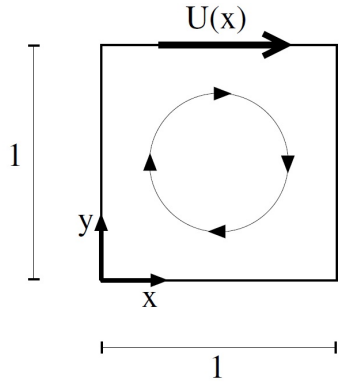

Figure 3. Polymer flow in a lid-driven cavity.

3.2 Numerical Implementation

The numerical implementation was made using the projection method in conjunction with a staggered grid. In the staggered grid, the velocities u and v and the pressure, p, are positioned in different places, according to the fig. 4.

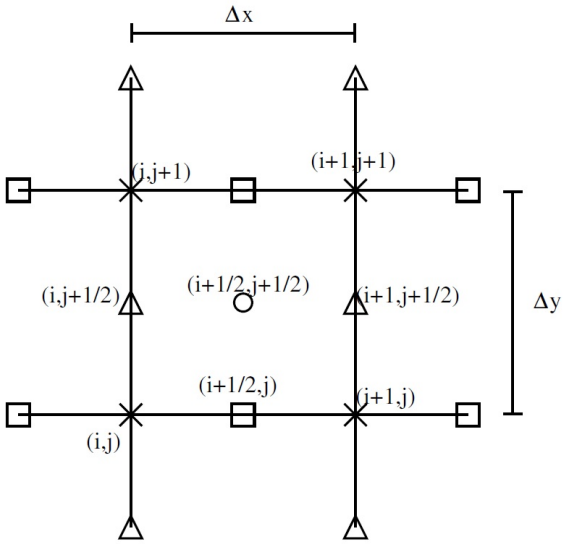

Figure 4. Staggered grid cell. Triangle: u component. Square: v component. Circle, pressure, p.

The model is based on three principal matrices, u, v and p. The dimensions are $u[0 : nx, -1 : ny]$, $v[-1 : nx, 0 : ny]$, $p[-1 : nx, -1 : ny]$. The physical position of u, is on the point $u(x, y) = u(i\Delta x, j\Delta y + \frac{1}{2}\Delta y)$, and, the analogous position in the u matrix would be $u[i, j]$. This way, the correlation for the other variables can be expressed folling the same pattern

$$u[i, j] \leftarrow u^k_{i,j+\frac{1}{2}} \tag{17}$$

$$v[i, j] \leftarrow v^k_{i+\frac{1}{2},j} \tag{18}$$

$$u_{star}[i, j] \leftarrow u^*_{i,j+\frac{1}{2}} \tag{19}$$

$$v_{star}[i,j] \leftarrow v^{*}_{i+\frac{1}{2},j} \tag{20}$$

$$u_{new}[i,j] \leftarrow u^{k+1}_{i,j+\frac{1}{2}} \tag{21}$$

$$v_{new}[i,j] \leftarrow v^{k+1}_{i+\frac{1}{2},j} \tag{22}$$

$$p[i,j] \leftarrow p^{k}_{i+\frac{1}{2},j+\frac{1}{2}} \tag{23}$$

$$D[i,j] \leftarrow D^{k}_{i+\frac{1}{2},j+\frac{1}{2}} \tag{24}$$

The non-dimensional viscosity, D, occupies the same place of the pressure in the grid. In this mesh, $dx = \frac{1}{nx}$ and $dy = \frac{1}{ny}$, the constants nx e ny being the number of divisions of the mesh, in the x and y directions, respectively. It is possible to notice that there is some values of *u, v* and p out of the physical domain, those point are denominated ghost points, used to impose the boundary conditions.

The following equations show the calculation in upper and bottom walls, for u and the left and right walls, for v, using the ghost points. The average between the points around the wall is the speed in the wall. In the other cases, that there is no ghost points, it can be calculated directly, because the components already are on the wall.

$$\frac{u[i,ny+1]-u[i,ny]}{2} = u_0 \tag{25}$$

$$\frac{u[i,0]-u[i,-1]}{2} = 0 \tag{26}$$

$$\frac{v[-1,j]-v[0,j]}{2} = 0 \tag{27}$$

$$\frac{v[nx+1,j]-v[nx,j]}{2} = 0 \tag{28}$$

The values of pressure in the borders are calculated using the ghost points, as exemplified below. For the left wall,

$$\frac{p_{-1,y}-p_{0,y}}{dx} = 0. \tag{29}$$

3.3 Code Attributes

The platform used to run the code is Spyder, an open source and platform for scientific programming, in Python language. The first-order projection method used in this paper, has a first-order error in time and second-order error in space. Most of the results presented in this paper are made for a final time of 60 seconds and a mesh size of $40x40$. The tool *streamplot* was used to plot the streamlines, the colors in the graphics are obtained directly, through the streamline equations.

The staggered grid was adopted because of the low efficiency of the traditional grid, in which the pressure is calculated by an average of odds and even positions in the grid, causing a non-physical oscillation in the values.

4 Code validation with benchmark results

In the present study, the incompressible non-Newtonian flow in a lid-driven cavity is solved using the projection method. The behavior of the flow are strongly affected by the Reynolds number and the power-law index. The circulation pattern and vortex formation are physical characteristics that allow a visual comparison to benchmark works made for different power-law index and Reynolds number found in literature. The code was first validated for Newtonian fluids. The visual comparison between the obtained data and the work of Ghia [4] can be done with the examples in the figures 5 and 6.

It can be seen the rising of circulation zone in both bottom corners and a curvature in the flow towards the left wall, when approaching the lid. The simulation was made for a final time of 60 seconds, a mesh size of $40x40$ and a constant viscosity.

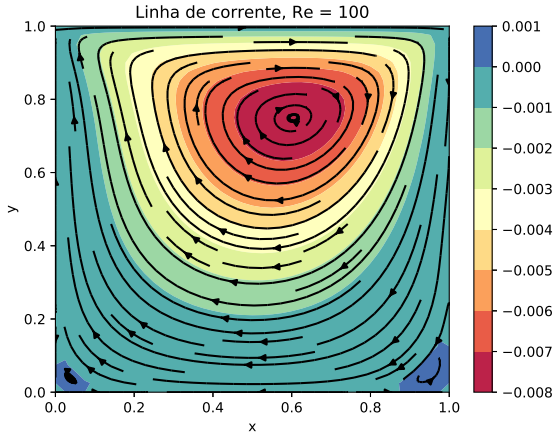

Figure 5. Numerical simulation, $Re = 100$.

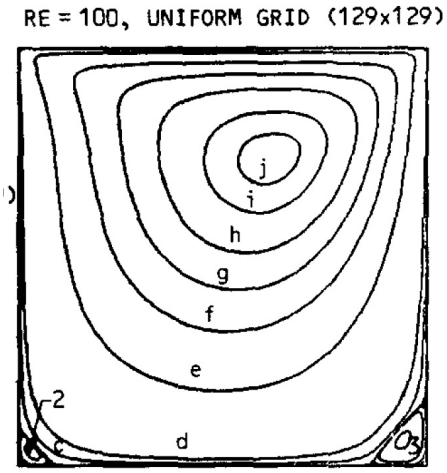

Figure 6. Lid-driven cavity flow, Newtonian fluid, $Re = 100$, image from Ghia [4].

5 Result and Discussions

Using the mathematical approach described in the methodology, the velocity equations of the first code were changed, with proper modifications. The development of the velocities changes the local dimensionless viscosity value, allowing new circulation patterns, vortexes and curves do compare.

For a value of the power law index $n = 1$, the results must be the same as a the results provided by the Newtonian fluid model. The fig. 7 shows the result for a simulation with $Re = 400$ and $n = 1$ and fig. 8 is the solution presented in the work of Ghia [4].

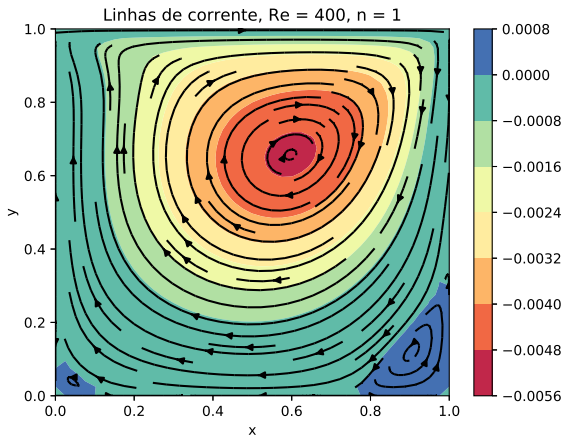

Figure 7. Numerical simulation, $Re = 400$, $n = 1$.

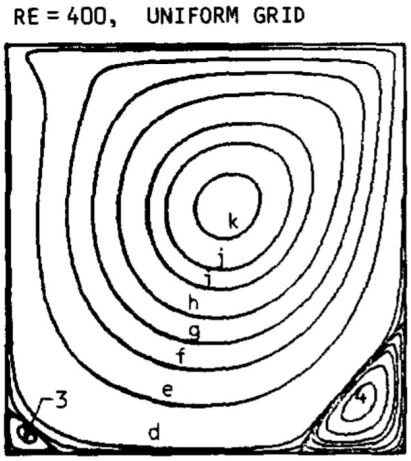

Figure 8. Lid-driven cavity flow, Newtonian fluid, $Re = 400$, image from Ghia [4].

The streamlines were obtained with the *streamplot* function. The streamline function creates some disturbances close to the wall, corners and zones with high concentration of lines. The arrows and lines must be used to determine the direction of the flow. The colors in fig. 7 describe the zones of the streamlines, obtained without pre-developed tools.

6 Conclusions

The model has short processing time and is light, made for the PYTHON Spider plataform. It was able to simulate, with a satisfactory precision, the behavior of a non-Newtonian fluid, allowing us to see the behavior of the viscosity with shear-thickening and shear-thinning characteristics.

The governing Navier-Stokes equations were evolved form the primitive variables formulation. They were non-dimensionalized through proper transformations. The dimensionless form of this equations were treated in a Cartesian coordinates to simulate the polymer behavior in the simplified geometry, the equations were then discretized using finite differences method. The computational model calculation is based in three steps, calculation of u^*, p and then the real velocity u, for each step of time. For permanent regime, the final time adopted was 40 seconds. The mesh has a $40x40$ size in the traditional grid.

Before to proceed with the non-Newtonian fluid model, the code was validated for a Newtonian model, as seen previously. We were able to notice the influence of successive over relaxation (SOR) in the time elapsed in calculations and a slightly discordance between the results and literature, for a high value Reynolds number.

Authorship statement. The authors hereby confirm that they are the sole liable persons responsible for the authorship of this work, and that all material that has been herein included as part of the present paper is either the property (and authorship) of the authors, or has the permission of the owners to be included here.

References

[1] Chorin, A. J., 1968. Numerical solution of the navier-stokes equations. In *Mathematics of Computation*.

[2] Richard, S. M. & Pearson, J. R. A., 1983. *Computational Analysis of Polymer Processing*. Springer Netherlands.

[3] Molla, M. M. & Yao, L., 2009. Non-newtonian natural convection along a vertical heated wavy surface using a modified power-law viscosity model. *Journal of Heat Transfer*.

[4] Ghia, U., G. K. S. C., 1982. High-re solutions for incompressible flow using the navier-stokes equations and a multigrid method. *Journal of Computational Physics*.